

# INCREMENTAL FATIGUE DAMAGE MODEL: APPLICATION TO PLANE PROBLEMS WITH NON-PROPORTIONAL LOADING

Zlatan Kapidžić<sup>1,2</sup>, Stefan B. Lindström<sup>2</sup> & Jonas Lundgren<sup>1</sup>

<sup>1</sup>Saab AB, SE-581 88 Linköping, Sweden

<sup>2</sup>Division of Solid Mechanics, Linköping University, SE-581 83 Linköping, Sweden

## Abstract

Modern airframe aluminum structures are increasingly manufactured in large and complex integral parts. Such parts are often exposed to in-plane, non-proportional loading and contain stress-raisers with complex geometry. Conventional methods, based on the stress concentration factor and cycle counting, are unsuitable for assessment of this type of problem. We present a fatigue damage model, based on the concept of moving endurance surface and incremental damage evolution. The fatigue damage is entirely dependent on the local stress history and the notch effect is accounted for by introduction of the relative stress gradient. Also, we present an automated and efficient implementation of the model, for the purpose of computing fatigue damage at stress raisers in plane problems with non-proportional loading. We demonstrate the implementation by an example of a fatigue calculation in an aircraft frame.

**Keywords:** Multiaxial fatigue, Non-proportional loading, Stress raisers

## 1. Introduction

The progressive enhancement of machining technique has made it feasible to efficiently manufacture large integral aluminum parts. Structural airframe parts, such as large frames, are thus possible to make in one piece, thereby reducing the number of parts compared to an assembled structure. Another advantage is that complex geometries can be integrated to facilitate weight reduction. On the other hand, heavily integrated structures are difficult to inspect, repair or replace in case of fatigue damage or failure. To avoid such problems, the fatigue assessment methods and models must be reliable and advanced enough in order to take into account the geometry, material and load complexities in integrated structures. Traditional fatigue assessment methods, using cycle-counting methods, uniaxial stress assumptions and simple notch criteria may be oversimplifying and misleading in such cases.

In this paper we consider a multiaxial, incremental fatigue damage model proposed by Ottosen et al. [1], which is based on the concept of moving endurance surface in stress space. The fatigue damage is integrated over the stress history, which alleviates the need for cycle counting. The original model was enhanced to consider stress concentrations by Ottosen et al. [2] and was further developed for non-proportional loading of aluminum by Lindström [3] and Lindström et al. [4]. Further modifications to the endurance surface, and considerations of stress concentrations and variable amplitude loading of aluminum, were introduced in [5].

Although the model is fully capable of handling general stress states and histories, we restrict the scope of this paper to plane problems with arbitrary in-plane stress raisers and non-proportional applied in-plane loading. We intend to demonstrate an automated and efficient implementation of a method for the solution of this complex problem. The implementation of the method has great potential for fast fatigue assessment of fatigue critical points in plane parts of integral aircraft frames.

## 2. Plane stress problem

We consider the plane stress problem for a linear elastic isotropic material, in the domain  $\Omega$  with the outer boundary  $\Gamma$ , as shown in Fig. 1. The domain contains  $k$  number of holes with boundaries  $H_k$ , where stress concentrations occur and which are therefore potentially fatigue critical points. Several load cases,  $i$ , are applied to the problem, where the traction  $\sigma_{\Gamma,i}(t)$  on the boundary varies over time  $t \in [0, T]$ . We assume that the boundary stresses may vary non-proportionally over time, resulting in variable locations and levels of the stress maximum along  $H_k$ . Although the stress state along  $H_k$  is uniaxial at every time instance, it can not be represented by an equivalent stationary cyclic case with a constant stress concentration factor. Conventional methods, which are based on a constant stress concentration factor, are therefore inadequate for fatigue assessment of this problem.

Due to the principle of superposition, the solution for each load case  $i$ , can be obtained as a linear combination of the solutions of the unit load cases. Since the time variation of the boundary stresses is assumed to be known, the solution  $\sigma(x, t)$  in every point  $x$  in the domain and at the boundaries  $H_k$ , over time, is obtained. The solution is the input to the fatigue model.

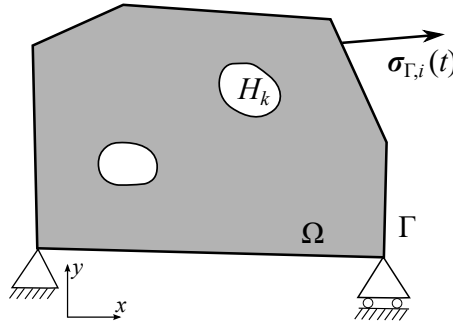


Figure 1 – Plane stress problem.

## 3. Fatigue model

The fatigue model is based on integration of a continuous-time stress history and on the concept of a moving endurance surface in stress space [1]. We introduce the endurance surface in stress space defined by

$$\beta(\bar{\sigma}, I_1) = 0 \quad (1)$$

where

$$\bar{\sigma}(\sigma, \alpha) = \sqrt{\frac{3}{2}} \|s - \alpha\| \quad (2)$$

is the effective stress,  $\alpha$  is the backstress tensor,  $s = \sigma - \frac{1}{3}\text{tr}(\sigma)\mathbf{I}$  is the deviatoric stress tensor and  $I_1 = \text{tr}(\sigma)$  is the first stress invariant. We specify the endurance surface by introducing an endurance function

$$\beta(\mathbf{y}) = \mathbf{y}^T \mathbf{A} \mathbf{y} + \mathbf{a}^T \mathbf{y} - 1, \quad \mathbf{y} = \frac{1}{E} \begin{bmatrix} \bar{\sigma} \\ I_1 \end{bmatrix} \quad (3)$$

where  $\mathbf{A}$  and  $\mathbf{a}$  are model parameter matrix and vector, respectively, and  $E$  is the Young's modulus. The evolution of the backstress allows for the movement of the endurance surface. The damage is measured by the variable  $D(t)$ , that is equal to 1 at failure. Initially, the damage and the backstress are zero, i.e.  $D(0) = 0$  and  $\alpha(0) = 0$ . The evolution of the damage and of the backstress are defined by the following rate equations

$$\begin{aligned}\dot{\alpha} &= C(s - \alpha)H(\beta)\langle\dot{\beta}\rangle \\ \dot{D} &= g(\beta)H(\beta)\langle\dot{\beta}\rangle\end{aligned}\quad (4)$$

where  $H(x)$  is the Heaviside step function, the Macaulay brackets  $\langle\cdot\rangle$  denote a ramp function,  $g(\beta) = Ke^{L\beta}$  is the damage function, and  $C$ ,  $K$  and  $L$  are material parameters. Both rates are non-zero only if  $\beta \geq 0$  and  $\dot{\beta} > 0$ , i.e. the endurance surface is moving and the damage develops only when the stress state is outside of the endurance surface and moving away from it. Following the variable substitution proposed in [4], we eliminate the implicit definition of  $\dot{\beta}$  from the rate equations by the substitution  $H(\beta)\langle\dot{\beta}\rangle = H(\beta)\langle v \rangle$  where

$$v(\sigma, \dot{\sigma}, \alpha) = \frac{1}{1 + C\bar{\sigma}\frac{\partial\beta}{\partial\bar{\sigma}}}\left[\sqrt{\frac{3}{2}}\frac{\partial\beta}{\partial\bar{\sigma}}\frac{(s - \alpha)}{\|s - \alpha\|} + \frac{\partial\beta}{\partial I_1}\mathbf{I}\right] : \dot{\sigma}\quad (5)$$

and where

$$\begin{bmatrix}\frac{\partial\beta}{\partial\bar{\sigma}} & \frac{\partial\beta}{\partial I_1}\end{bmatrix} = \frac{1}{E}(2\mathbf{y}^T\mathbf{A} + \mathbf{a}^T)\quad (6)$$

Substitution of Eq. (5) into Eq. (4) results in a set of ordinary differential equations which are solved using standard methods.

To account for the notch effect, we modify the endurance function by introduction of the relative stress gradient

$$\chi = \frac{\int_0^T |\nabla\sigma_{vM}| \|\dot{\sigma}\| dt}{\int_0^T \sigma_{vM} \|\dot{\sigma}\| dt}\quad (7)$$

where  $\sigma_{vM} = \sqrt{3/2}\|s\|$  is the von Mises stress, so that  $\beta(\bar{\sigma}, I_1, \chi)$ , as proposed in [5]. This is achieved by introduction of the diagonal matrix  $\boldsymbol{\mu}_\chi = \text{diag}[\mu_1(\chi), \mu_2(\chi)]$ , that is used to modify the model parameters in Eq. (3), so that  $\mathbf{A} = \boldsymbol{\mu}_\chi^T \mathbf{A}^0 \boldsymbol{\mu}_\chi$  and  $\mathbf{a} = \boldsymbol{\mu}_\chi^T \mathbf{a}^0$ , where  $\mathbf{A}^0$  and  $\mathbf{a}^0$  are the parameters of the homogeneous stress state. The stress reduction functions are chosen as, see [5],

$$\mu_1(\chi) = \mu_2(\chi) = \frac{1 + \mu_\infty \sqrt{\lambda\chi}}{1 + \sqrt{\lambda\chi}}\quad (8)$$

where  $\lambda$  and  $\mu_\infty$  are material constants. Totally seven parameters are fitted to constant amplitude tests on notched AA7050-T7 specimens in [5] and three parameters are set to fixed values,  $A_{11}^0 = 0$ ,  $A_{12}^0 = 0$  and  $C = 10$ . Table 1 shows the least-squares optimized values of the parameters. Validation of variable amplitude fatigue life against tests is also performed in [5].

Table 1 – Model parameters AA7050-T7.

$A_{11}^0$	$A_{12}^0$	$A_{22}^0$	$a_1^0$	$a_2^0$	$K$	$L$	$C$	$\lambda$ [mm]	$\mu_\infty$
0	0	-12700	501	180	$4.09 \cdot 10^{-5}$	12.9	10	9.7	0.626

#### 4. Implementation

The solution to the plane stress problem with non-proportional applied in-plane loading is implemented in a MATLAB-program, where a finite element (FE) program is utilized for the solution of the stress field. The program creates a plane geometry based on the outer shape of the domain, which can include circular, elliptic or smooth polygon shaped holes. An FE-mesh, with second-order, plane

stress elements is generated automatically in the program. Three load components are applied on the domain, normal distributed forces in  $x$ - and  $y$ -directions,  $N_{xx}$  and  $N_{yy}$  and a distributed shear force  $N_{xy}$ . These are total net loads applied on the domain and are achieved by application of normal and shear forces on the boundaries so that the equilibrium is obtained. A unit load case is solved for each load component resulting in the solutions  $\sigma_{xx}(\mathbf{x})$ ,  $\sigma_{yy}(\mathbf{x})$  and  $\sigma_{xy}(\mathbf{x})$ . Any combined load state is then obtained by superposition of the solutions for the three unit load cases. The time-history for each load component is given as reversal points at time points  $t_j$ , which are common for all load components, as shown in Fig. 4. The stress history is then given by

$$\sigma(\mathbf{x}, t_j) = \sigma_{xx}(\mathbf{x})N_{xx}(t_j) + \sigma_{yy}(\mathbf{x})N_{yy}(t_j) + \sigma_{xy}(\mathbf{x})N_{xy}(t_j) \quad (9)$$

Thereafter, the program uses the fatigue model to calculate the fatigue damage at all hole edges.

## 5. Example

We illustrate the usage of the MATLAB-program by an example of a fatigue damage calculation in a web section of a fighter aircraft fuselage frame. The frame geometry, shown in Fig. 2, is an integral aluminum structure consisting of a web, flanges and stiffeners. The web is compartmentalized by stiffeners into sections of different sizes and shapes, which may contain multiple holes. In this example, we focus on the web section indicated by the red arrow. The section is delimited by four stiffeners and contains a large hole surrounded by eight small holes, as shown in Fig. 2.

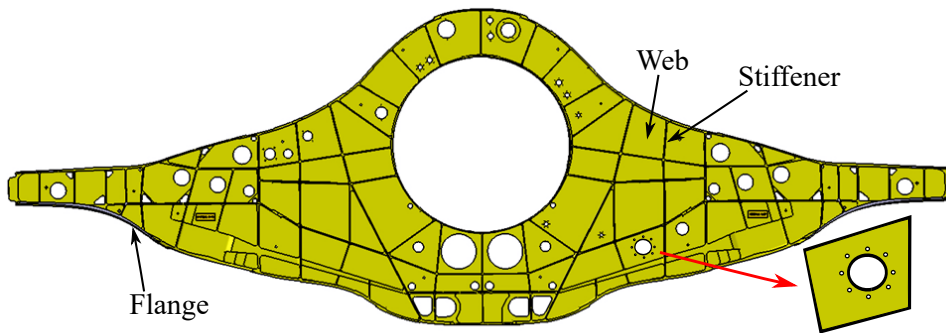


Figure 2 – Aircraft frame geometry.

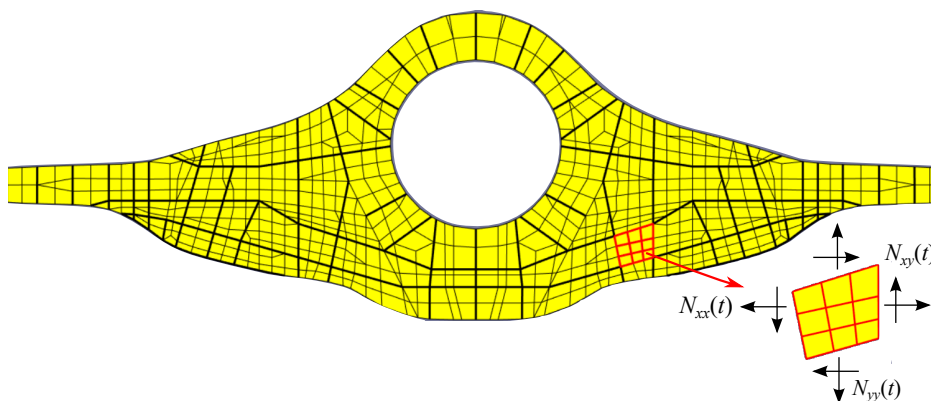


Figure 3 – FE-mesh of the frame in the global model.

A global FE-model of the entire aircraft is solved, for a large number of flight states, to compute the load distribution in the airframe structure. In the global model, the webs are represented by shell elements and the stiffeners and flanges are modeled with bars and beams. Figure 3 shows the global FE-mesh of the frame and the definition of the distributed forces that are applied on the web section. Note that the global FE-model has a very low resolution and that the holes are not included. For any element, or a group of elements, the load sequence for any force can be computed as a sequence of

combinations of the flight state solutions.

The normalized sequences, for the three distributed loads on the web section are shown in Fig. 4, where the top plot shows the entire duration of the sequence, while the bottom plot shows the first 150 states. From the bottom plot, it is evident that the loads, and therefore also the stress state cf. Eq. (9), vary non-proportionally.

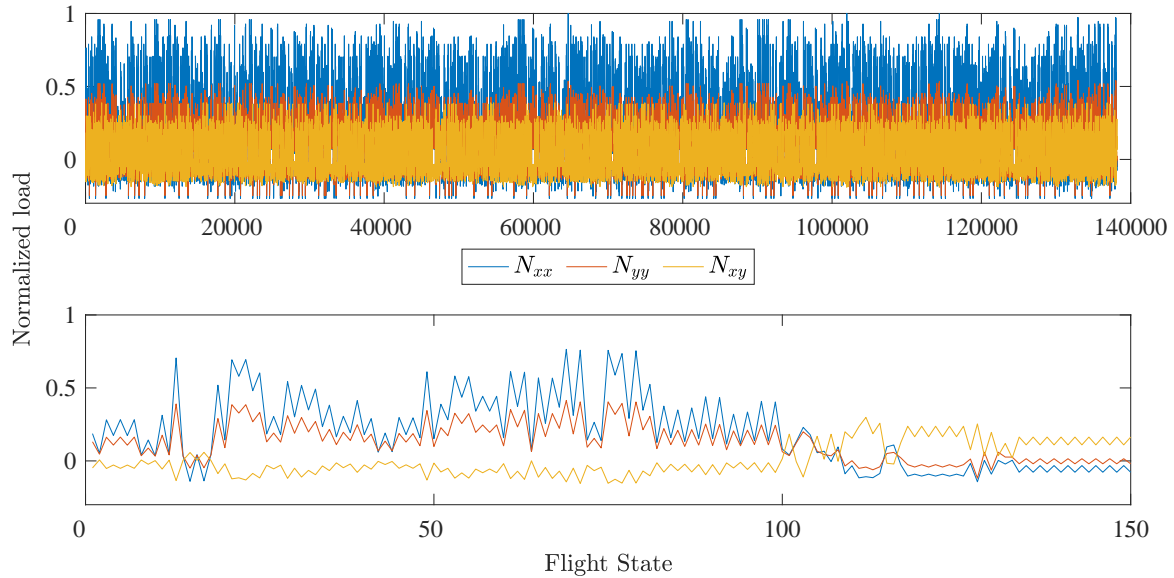


Figure 4 – Load sequences.

Next, we define the geometry of the web section, including the holes, by specifying the coordinates of each feature in the MATLAB-program. The outer edges are denoted E1–E4 and the holes are numbered H1–H9, see Fig. 5a. Thereafter, a mesh of second-order plane stress elements is created, see Fig. 5b. It is possible to control the mesh by, for instance, assigning the maximum element size.

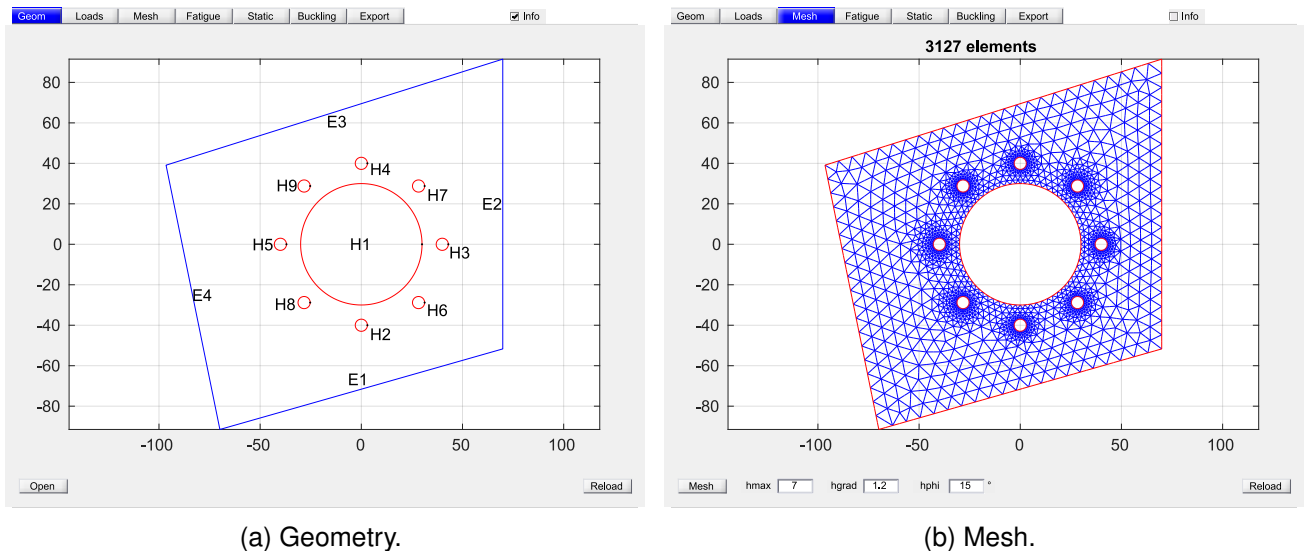


Figure 5 – Definition of the geometry and mesh in the MATLAB-program.

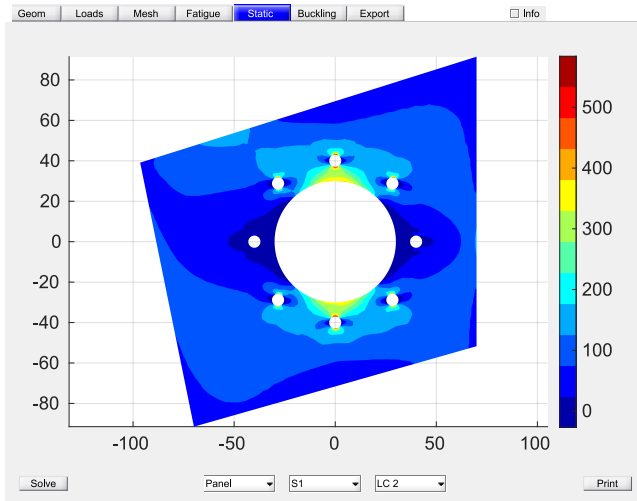
The loads are defined in a text file that contains the three sequences shown in Fig. 4 and is read by the program. The sequences can be scaled by assigning the maximum sequence level for each of the load components  $N_{xx}$ ,  $N_{yy}$  and  $N_{xy}$ . Also, several calculations can be defined and run at once. Given the maximum levels of the load components, the program calculates the normal and shear distributed forces  $N$  and  $S$  to be applied on the edges, in order to achieve the force and moment equilibrium for every unit load case. Table 2 shows the normalized edge forces for the unit load cases

### Incremental fatigue damage model: Application to plane problems with non-proportional loading

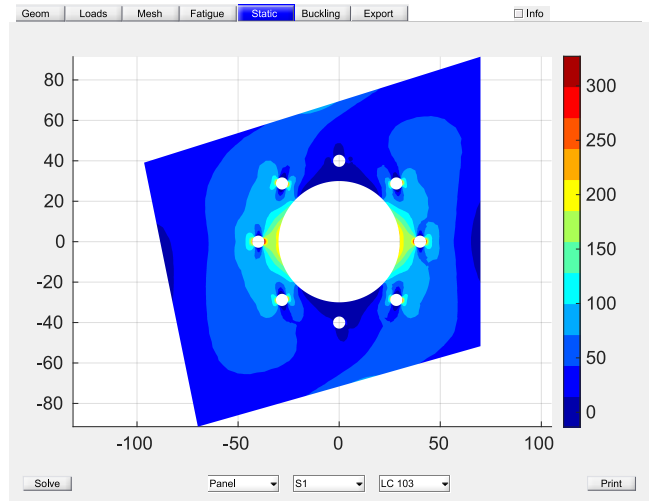
in the current example. The model is restrained at one corner point and solved for the three unit load cases. No other restrictions are applied to the outer edge displacements. The resulting stress field at maximum sequence levels can be plotted, either for individual load cases as shown in Fig. 6, or for a combined load case. Using the three solutions and the load sequences with Eq. (9), the stress history is calculated along all hole edges. The out-of-plane stress components are zero. Finally, the fatigue damage is calculated along all hole edges using the fatigue model.

Table 2 – Normal and shear edge forces for the unit load cases (ULC).

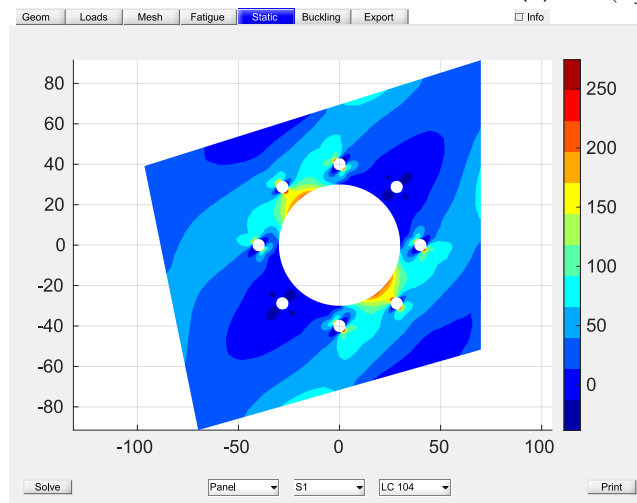
ULC		E1	E2	E3	E4
$N_{xx} = 1$	$N$	0.07	1.00	0.09	0.96
	$S$	0.26	0.00	0.29	-0.20
$N_{yy} = 1$	$N$	0.93	0.00	0.91	0.04
	$S$	-0.26	0.00	-0.29	0.20
$N_{xy} = 1$	$N$	-0.53	0.00	-0.57	0.39
	$S$	-0.86	1.00	-0.82	0.92



(a)  $\max(N_{xx}) = 124.6 \text{ N/mm}$



(b)  $\max(N_{yy}) = 67.7 \text{ N/mm}$



(c)  $\max(N_{xy}) = 48.3 \text{ N/mm}$

Figure 6 – First principal stress (MPa) at maximum sequence load levels for each load component.

In this example, we compute the fatigue damage for two cases of loading: 1) a case with all three load

components active ( $N_{xx}, N_{yy}, N_{xy}$ ) as shown in Fig. 4, and 2) a case where only the  $N_{xx}$  component is active ( $N_{xx}, 0, 0$ ). The damage over the normalized edge length for all holes is shown in Fig. 7a. The normalized edge length is measured counter clockwise from a point located at three o'clock at every hole edge. For both case 1 and 2, the maximum damage occurs at hole H4 and the damage is larger in case 2, were only  $N_{xx}$  is applied, see also Fig. 7c. At the neighboring hole H7, case 1 gives the largest damage, see Fig. 7d. At the large center hole H1, the damage is relatively low and has four local maxima along the edge, due to the proximity of the satellite holes. The program also calculates the number of flight hours that correspond to a given allowed damage sum.

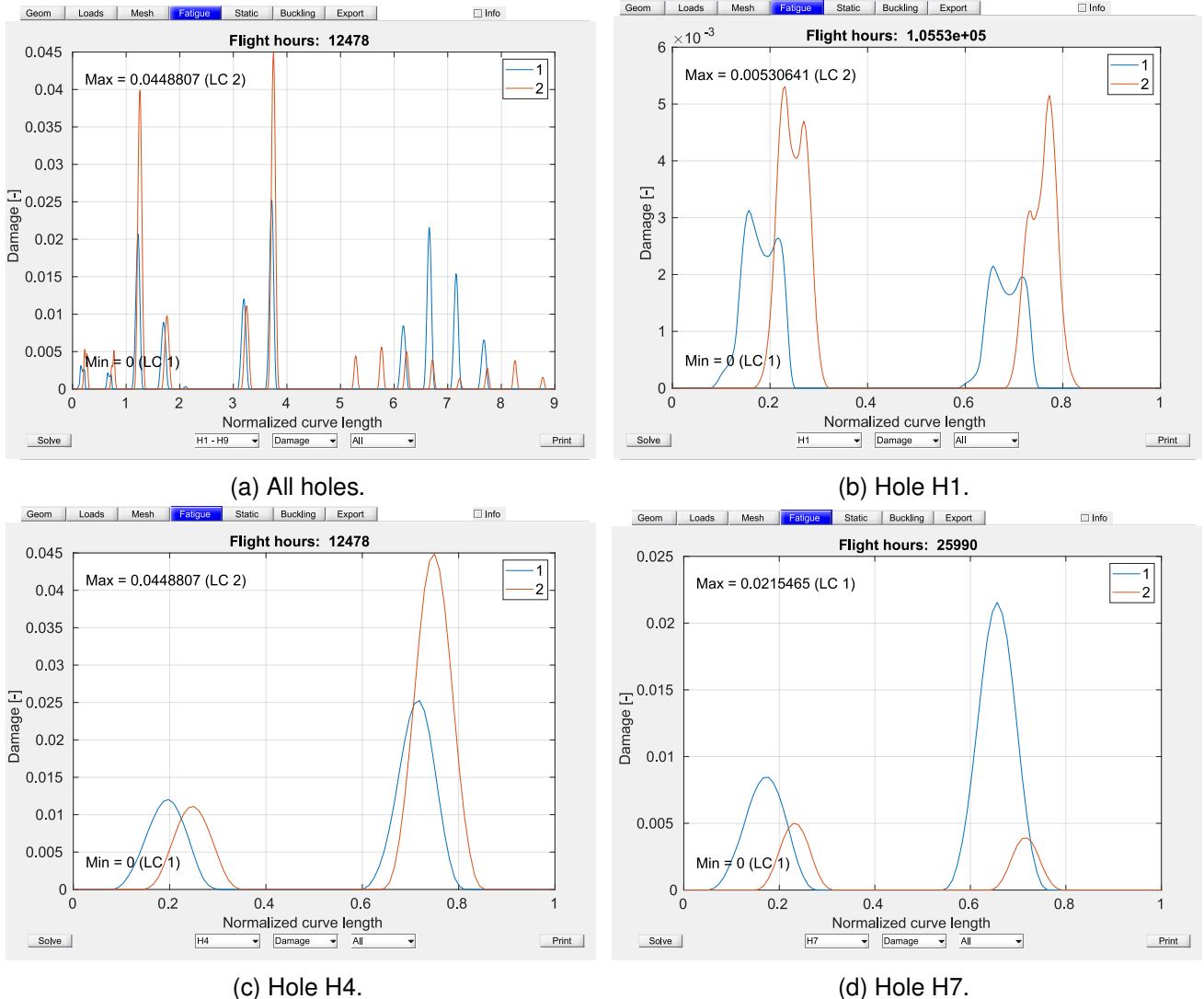


Figure 7 – Damage along the normalized edge length.

## 6. Conclusions

The paper presents a previously developed incremental fatigue damage model and its implementation for solution of plane problems with non-proportional loading. The usage of the implemented program is demonstrated by an example of a calculation of fatigue damage in an aircraft frame. Since the model is based entirely on integration of the local stress field history, it has an advantage over conventional approaches which are based on the stress concentration factor and cycle counting methods, both of which are ambiguous concepts in the current problem. The proposed model and the demonstrated implementation facilitate an efficient fatigue calculation process that can be automated for the purpose of performing numerous runs. It is particularly useful for design of the placement and shape of the stress-raisers in plane aircraft frame structure.

## 7. Contact Author Email Address

Email the corresponding author at: zlatan.kapidzic@saabgroup.com.

Email the co-authors at: stefan.lindstrom@liu.se and jonas.lundgren@saabgroup.com.

## 8. Copyright Statement

The authors confirm that they, and/or their company or organization, hold copyright on all of the original material included in this paper. The authors also confirm that they have obtained permission, from the copyright holder of any third party material included in this paper, to publish it as part of their paper. The authors confirm that they give permission, or have obtained permission from the copyright holder of this paper, for the publication and distribution of this paper as part of the ICAS proceedings or as individual off-prints from the proceedings.

## References

- [1] Ottosen NS, Stenström R and Ristinmaa M. Continuum approach to high-cycle fatigue modeling. *International Journal of Fatigue*, Vol. 30, No. 6, pp 996–1006, 2008.
- [2] Ottosen NS, Ristinmaa M and Kouhia R. Enhanced multiaxial fatigue criterion that considers stress gradient effects. *International Journal of Fatigue*, Vol. 116, pp 128–139, 2018.
- [3] Lindström SB. Continuous-time, high-cycle fatigue model for nonproportional stress with validation for 7075-T6 aluminum alloy. *International Journal of Fatigue*, Vol. 140, pp 105839, 2020.
- [4] Lindström SB, Thore CJ, Suresh S and Klarbring A. Continuous-time, high-cycle fatigue model: Validity range and computational acceleration for cyclic stress. *International Journal of Fatigue*, Vol. 136, pp 105582, 2020.
- [5] Lindström SB, Moverare J, Leidermark D, Ansell H, and Kapidžić Z. Incremental fatigue damage modeling of 7050-T7 aluminum alloy at stress-raisers. *International Journal of Fatigue*, Vol. 161, pp 106878, 2022.